

Photochemical & Photobiological Sciences

Accepted Manuscript



This is an *Accepted Manuscript*, which has been through the Royal Society of Chemistry peer review process and has been accepted for publication.

Accepted Manuscripts are published online shortly after acceptance, before technical editing, formatting and proof reading. Using this free service, authors can make their results available to the community, in citable form, before we publish the edited article. We will replace this *Accepted Manuscript* with the edited and formatted *Advance Article* as soon as it is available.

You can find more information about *Accepted Manuscripts* in the [Information for Authors](#).

Please note that technical editing may introduce minor changes to the text and/or graphics, which may alter content. The journal's standard [Terms & Conditions](#) and the [Ethical guidelines](#) still apply. In no event shall the Royal Society of Chemistry be held responsible for any errors or omissions in this *Accepted Manuscript* or any consequences arising from the use of any information it contains.

Photochemical reactions of halogenated aromatic 1,3-diketones in solution studied by steady state, one- and two-color laser flash photolyses

Minoru Yamaji,^{a,*} Yurie Suwa,^b Rieko Shimokawa,^b Cecilia Paris^c and Miguel Ángel Miranda^{c,*}

^a *Division of Molecular Science, Graduate School of Science and Technology, Gunma University, Kiryu, Gunma 376-8515, Japan*

^b *Education Program of Materials and Bioscience, Graduate School of Science and Engineering, Gunma University, Kiryu, Gunma 376-8515, Japan*

^c *Instituto de Tecnología Química UPV-CSIC, Universidad Politécnica de Valencia, Valencia, Spain*

E-mail: yamaji@gunma-u.ac.jp (M. Yamaji), mmiranda@qim.upv.es (M.A. Miranda)

Abstract

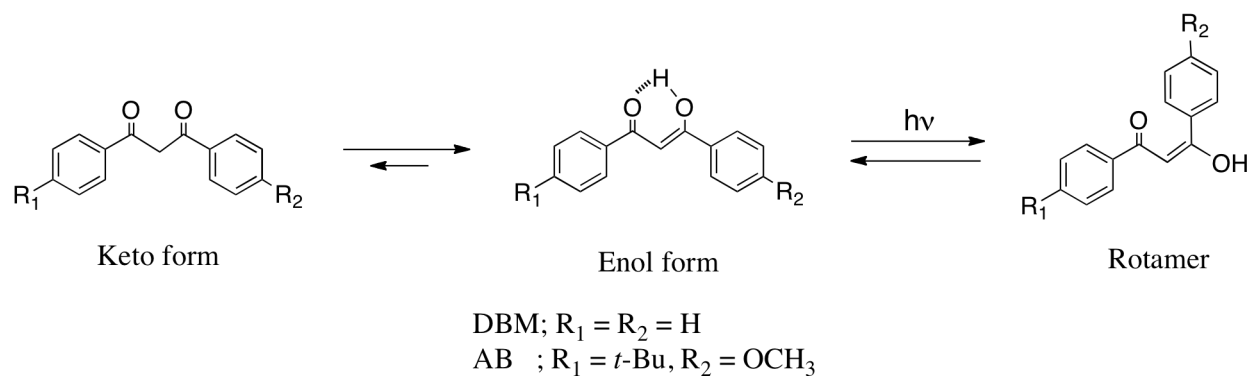
Photochemical processes of 4-*tert*-butyl-4'-methoxydibenzoylmethane (avobenzene, AB), 4-phenylbenzoylbenzoyl-, 4-phenylbenzoyl-2'-furanlyl- and 4-phenylbenzoyl-2'-thenoylmethanes (PB@Ph, PB@F and PB@T, respectively) substituted with Br and Cl at the C2 position were studied by stationary and laser flash photolyses in solution. The absorption spectral features showed that the molecular structures of the halogenated diketones are in the keto forms while those of halogen-free diketones are in the enol forms. The excited singlet and triplet state energies were determined from the absorption and emission spectra. From the absorption spectral changes upon steady state photolysis of brominated diketones in ethanol, the corresponding halogen-free diketone due to Br elimination was found to be the major photochemical process. The determined quantum yields for the formation of the halogen-free diketones were independent of the amount of the dissolved oxygen, indicating that the elimination process is the event in the excited singlet (S_1) states. In contrast, from the observed absorption spectra obtained upon photolysis of chlorinated AB and PB@Ph, it was inferred that Norrish type I is the major photochemical reaction in the S_1 states in acetonitrile. Chlorinated PB@F and PB@T were found to undergo Cl elimination in the S_1 states in cyclohexane to form the corresponding halogen-free diketones. Laser photolysis studies of brominated AB in acetonitrile and ethanol provided a transient absorption spectrum ascribable to the avobenzene radical (ABR) produced by debromination as the initial intermediate, followed by the

AB formation in ethanol. The quenching rate constant of ABR by ethanol and the quantum yield of the AB formation via ABR were determined. These observations provided evidence that H-atom abstraction of ABR from ethanol is responsible for the AB formation. Conversely, laser flash photolysis of brominated and chlorinated PB@Ph, PB@F and PB@T demonstrated the formation of the triplet-triplet absorption. No chemical reactions were found to occur in the triplet (T_1) states. Two-color two-laser photolysis studies were carried out on the T_1 state of chlorinated PB@Ph, PB@F and PB@T, resulting in the formation of the corresponding halogen-free diketones. These observations convinced occurrence of Cl elimination in the highly excited triplet (T_n , $n \geq 2$) states. Based on the computed bond dissociation energies for the C-halogen and C-C bonds, switching mechanisms of dehalogenation and α -cleavage were discussed.

* Authors to whom correspondence should be addressed.

1. Introduction

Keto-enol tautomerizations of aromatic alkenes in solution are typical chemical processes in a thermal equilibrium. 1,3-Dibenzoylmethane (DBM), a typical representative of the β -dicarbonyl compounds, takes an enol form as the molecular configuration at room temperature. Enol forms of DBMs have strong absorption bands in the UVA region (315-380 nm) originated from the π - π^* transition of the chelated quasi-aromatic π -electron system. As most of DBMs are nonfluorescent in solution, the presence of efficient nonradiative processes from the excited singlet states is indicative. In fact, this process has been revealed to involve the formation of transient enol isomers (rotamers) followed by recovery to the chelated enol form in the dark. The tautomerization and isomerization processes of DBMs are shown in Scheme 1.



Scheme 1. Keto-enol tautomerization of DBMs and isomerization processes of enol DBMs.

DBMs are, therefore, applicable to UVA sunlight screening. Practically, 4-*tert*-butyl-4'-methoxydibenzoylmethane (trade name, Avobenzone, here abbreviated as AB) is one of the most widely used UVA sunscreen. There are an amount of reports for understanding and utilizing photochemical and photophysical properties of AB.¹⁻²⁰ Because AB has large absorbance at 350 nm, the molecular structure of AB in the ground state is the enol form. Photochemical behavior of AB is almost the same as that of DBM (Scheme 1) whereas AB is shown to photodecompose via the Norrish type I mechanism.^{4,5}

We have reported photochemical features of alkylated ABs. Methylated AB (1,1-(4-*tert*-butylbenzoyl)(4'-methoxybenzoyl)ethane; MeAB) shows large absorption in the UVC region (200 - 280 nm) because the methyl group hinders the keto form of DBM moiety tautomerizing to the enol form in the ground state.¹⁸ Laser photolysis investigations of MeAB revealed the efficient formation of the triplet state via a fast intersystem crossing from the excited singlet state of the keto-formed MeAB. Propylated AB (1,1-(4-*tert*-butylbenzoyl)(4'-methoxybenzoyl)butane) in the keto form was shown to undergo the Norrish type II reaction in the n,π^* triplet state in solution.²¹ These photophysical features of triplet keto-formed ABs are similar to that of carbonyl aromatic compounds, such as benzophenone whose electronic character of the triplet state is of an n,π^* type. It seems that introduction of substituent groups to the AB skeleton allows the formation of n,π^* triplets upon photoexcitation of the keto-formed ABs. When the phenyl group of benzophenone is replaced with larger π -electron systems, such as biphenyl and naphthyl moieties, it is reported that the electronic character of the lowest triplet (T_1) state changes from n,π^* to π,π^* , and the triplet

energy level decreases.²² It is of our interest what differences emerge in their photochemical and photophysical properties when π -electron moieties different from the phenyl ring are introduced in the 1,3-diketone backbone.

In the present study, we prepare AB derivative halogenated at the C2 position (4-*tert*-butyl-4'-methoxydibenzoylbromomethane; BrAB and 4-*tert*-butyl-4'-methoxydibenzoylchloromethane; ClAB) that is expected to be in keto forms in the ground state. We have also prepared 4-phenylbenzoyl benzoyl- (PB@Ph), 4-phenylbenzoyl furanyl- (PB@F), and 4-phenylbenzoyl theonylmethans (PB@T) by replacing the phenyl rings of DBM with biphenyl, furan and thiophene moieties, and their halogenated derivatives were prepared (see Chart 1 for the molecular structures and the abbreviations). By using steady state and laser flash photolysis techniques, the photophysical and photochemical features of halogenated DBM derivatives are investigated in solution.

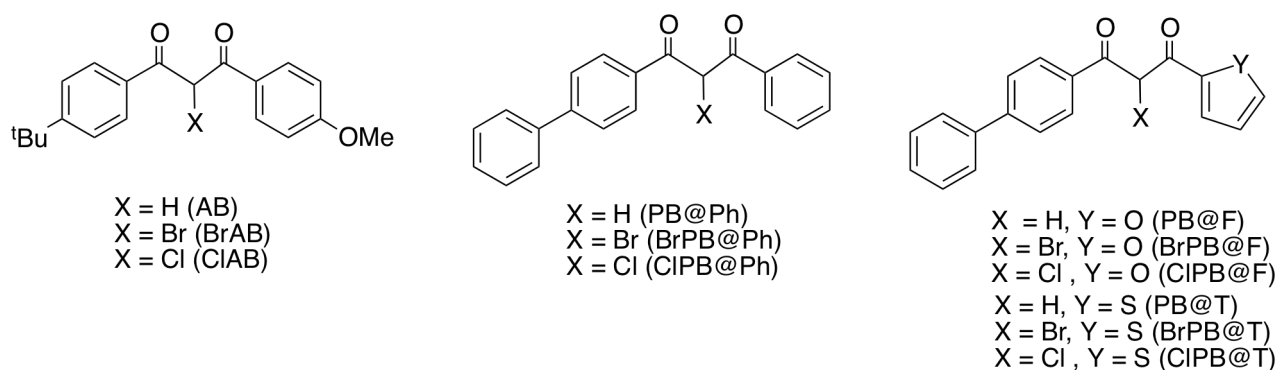


Chart 1. Molecular structures and abbreviations of the used compounds in this study.

2. Experimental

Avobenzene (AB; 4-*tert*-butyl-4'-methoxydibenzoylmethane, >99 % purity) was purchased from Fluka, and purified by recrystallizations from ethanol before the use. 4-Phenylbenzoyl benzoylmethane (PB@Ph) was prepared according the literature.²³ Bromoavobenzene (4-*tert*-butylbenzoyl-4'-methoxybenzoylmethane; BrAB) and bromo(4-phenylbenzoyl)benzoylmethane (BrPB@Ph) were prepared according to the same procedure for dibenzoylbromomethane.²⁴ Chloroavobenzene (4-*tert*-butylbenzoyl-4'-methoxybenzoylchloromethane; ClAB) and chloro(4-phenylbenzoyl)benzoylmethane (ClPB@Ph) were prepared by the same procedure for 2-chloro-1,3-

diarylpropan-1,3-diones.²⁵ The preparation procedures and the NMR data of BrPB@Ph, CIPB@Ph, PB@F, PB@T, BrPB@F, BrPB@T, CIPB@F and CIPB@T are deposited in the electronic Supplementary Information (ESI). *N*-Methyldiphenylamine (MDPA) from Tokyo Kasei (TCI) was distilled under reduced pressure for purification before the use. Acetonitrile (ACN) was distilled for purification. Ethanol (EtOH, spectroscopic grade from Kishida), cyclohexane (CH, spectroscopic grade from Wako) and methylcyclohexane (MCH, photometric grade from Aldrich) were used without further purification.

Absorption spectra were recorded on a U-best 50 (JASCO) spectrophotometer whereas emission spectra were on a Hitachi F-4010 fluorescence spectrophotometer. Samples in a quartz cell with a 1 cm path length were prepared in the dark, and Ar-purged or degassed by several freeze-pump-thaw cycles on a high vacuum line when necessary. Steady state photolysis was carried out by using a low-pressure Hg lamp (254 nm) and a high-pressure Hg lamp with an cut-off filter at 295 K unless noted. The photon flux at 254 nm was determined by using *N*-methyldiphenylamine in aerated methylcyclohexane as a chemical actinometer. The quantum yield for the formation of *N*-methylcarbazole from *N*-methyldiphenylamine has been established as 0.42.²⁶ The procedure for determining quantum yields with the use of absorption spectrum changes was the same as that described in the literature.²⁷ Fourth harmonics (266 nm) from a Nd:YAG laser system (12 mJ / pulse, Lotis-TII, LT-2137), 430 nm (10 mJ / pulse) and 440 nm (7 mJ / pulse) laser pulses from a Ti:Sapphire laser system (Lotis-TII, LT-2211) pumped with second harmonics (532 nm) from the Nd:YAG laser system and a XeCl excimer laser (308 nm, 17 mJ /pulse, Lextra 50 from Lambda Physik) were used as the excitation laser light sources. The details of the detection system for the time profiles of the transient absorption have been reported elsewhere.²⁸ Transient absorption spectra were obtained using a Unisoku USP-T1000-MLT system, which provides a transient absorption spectrum with one laser pulse. The obtained transient spectral data were analyzed using the least-squares best-fitting method. The temporal data of absorbance changes were analyzed by using the least-squares best-fitting method. Density functional theory (DFT) calculations for heats of formation were performed using the Gaussian 09 program.²⁹

3. Results and Discussion

3.1 Absorption and emission measurements

Figure 1 shows absorption and emission spectra of AB, PB@Ph and the halogenated compounds in solution.

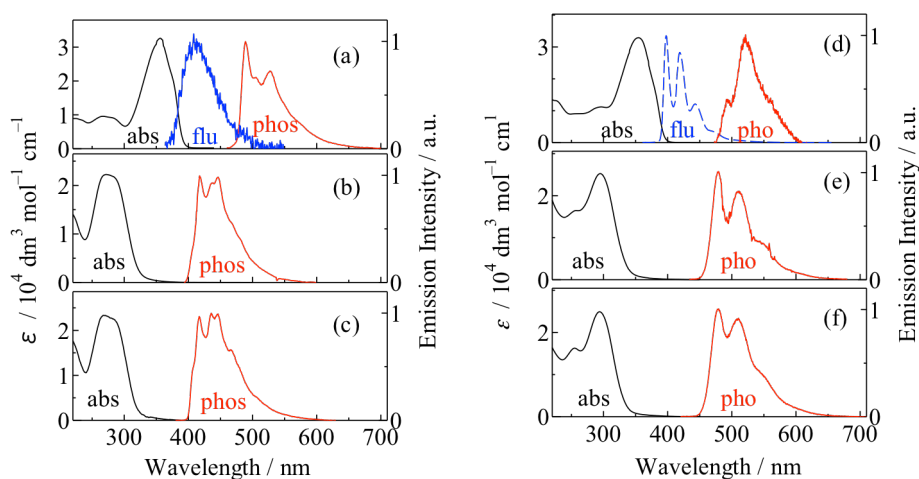


Figure 1. Absorption spectra (solid) in ACN at 295 K and phosphorescence spectra (res) in EtOH at 77 K for AB (a), BrAB (b), ClAB (c), PB@Ph (d), BrPB@Ph (e) and ClPB@Ph (f). Fluorescence (blue) was observed for AB in ACN at 295 K (a) and PB@Ph in EtOH at 77 K (d) while that from BrAB, ClAB, BrPB@Ph and ClPB@Ph was not observed at 295 K and 77 K.

The absorption band of AB is located at 356 nm indicating that AB takes the enol form in the ground state.⁶ Conversely, BrAB and ClAB show the absorption maxima at 260 - 270 nm, indicating that they take the keto form in the ground state. Very weak fluorescence from AB was recorded at 295 K while that from BrAB and ClAB was not observed under the same conditions. Similarly, from the wavelength region of the absorption bands, it is inferred that PB@Ph and the halogenated compounds take the enol and the keto forms, respectively. The absorption and emission features of PB@F, PB@T and the halogenated derivatives, whose spectra are deposited in the ESI (Figure S1), are very similar to those of PB@Phs. The observation and absence of fluorescence from the studied compounds indicate that the electronic character of the lowest excited singlet (S_1) state of the halogenated derivatives is of n,π^* while that of the enol-formed compounds is of π,π^* . It was confirmed that the excitation spectra of the emission agree well with the corresponding absorption spectra. Phosphorescence spectra of the studied compounds show vibrational structures due to the

carbonyl progression. The phosphorescence shapes of the enol forms and the halogenated diketones having biphenyl moiety are, respectively, similar irrespective of the other chromophores, indicating that the triplet energy is mainly localized on the biphenyl moiety and that the electronic character of the triplets is of π,π^* . The energy levels of the T_1 states were determined from the 0-0 origins of the phosphorescence spectra. The spectroscopic data of the used compounds are summarized in Table 1.

3.2.1 Photochemical features of brominated diketones in solution

Figure 2 shows absorption spectral changes upon photolysis of BrAB and BrPB@Ph in solution.

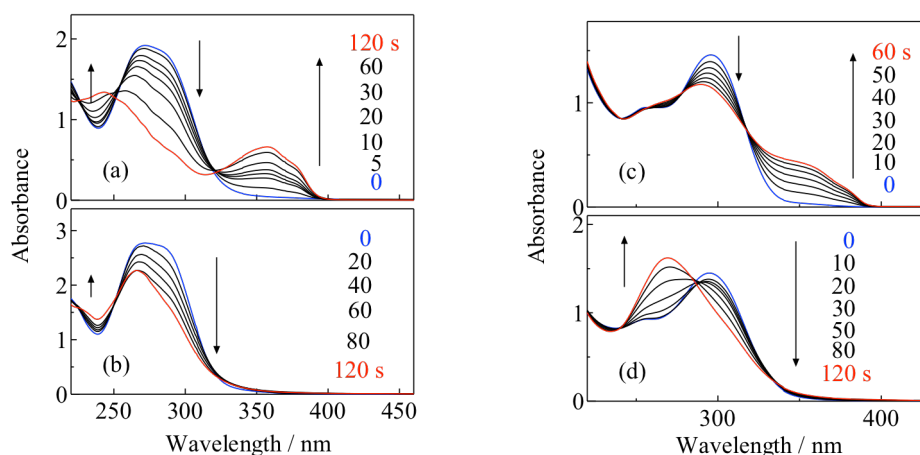
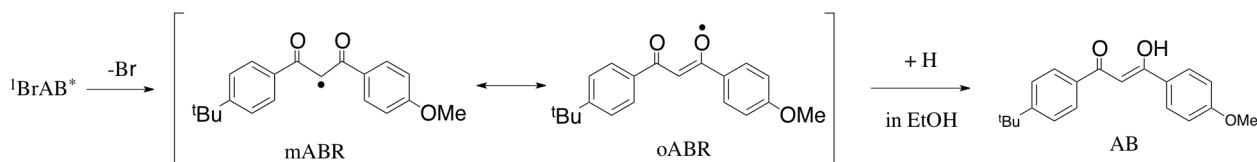


Figure 2. Absorption spectral changes upon photolysis of BrAB in degassed EtOH (a) and ACN (b), and BrPB@Ph in degassed CH (c) and ACN (d).

With an increase of 254 nm irradiation time, the intensity of the absorption band of BrAB at 270 nm decreased in EtOH while that at 356 nm increased with isosbestic points (Figure 2a). The emerged absorption band at 356 nm agrees with that of AB, indicating occurrence of photodebromination from BrAB forming the 4-*tert*-butyl-4'-methoxydibenzoylmethyl radical (ABR) that would undergo H-abstraction from EtOH. The conformations of ABR may be in either a methyl-radical or an oxy-radical form (denoted as mABR and oABR, respectively) both of which are mesomeric structures (Scheme 2).



Scheme 2. Photochemical formation of AB via ABR from photoexcited BrAB in EtOH.

Interestingly, photochemical features of BrAB in ACN were found to differ from that in EtOH. The absorption band of AB did not appear upon 254 nm photolysis of BrAB in ACN (Figure 2b) while a new absorption band appeared at 266 nm. We were unable to identify the photoproduct having the absorption at 266 nm. Similarly, upon photolysis ($\lambda > 280$ nm) of BrPB@Ph in CH, the absorption band at 295 nm diminishes with isosbestic points accompanying a developing absorption band at 354 nm (Figure 2c), which is similar to that of PB@Ph. These observations also demonstrate debromination in the excited state of BrPB@Ph. The quantum yields of the AB formation in EtOH and the PB@Ph formation on CH were determined to be 0.08 ± 0.01 and 0.10 ± 0.01 , respectively. Since these quantum yields were independent of the amount of dissolved oxygen, the debromination of BrAB and BrPB@Ph is considered to proceed in the S_1 state. Photolysis of BrPB@Ph in ACN provided definite absorption spectral changes with isosbestic points (Figure 2d) although the final absorption band at 268 nm were unable to be identified. We also investigated absorption spectral changes upon stationary photolysis ($\lambda > 280$ nm) of BrPB@F and BrPB@T in EtOH and CH (Figures S2 and 3 in the ESI). We have recognized that BrPB@T undergoes photodebromination in EtOH producing PB@T with a quantum yield of 0.10 ± 0.01 whereas BrPB@F showed strange absorption spectral changes in EtOH. Since absorption spectrum of BrPB@F in EtOH consisted of the absorption bands of the keto and the enol, we were unable to explain the photochemical reactions in EtOH. In CH, BrPB@F and BrPB@T seemed to decompose showing isosbestic points in the absorption spectral changes although the appeared absorption spectra were different from those of the corresponding enol forms. Photochemical reaction of BrPB@F and BrPB@T are strongly dependent on the variety of the solvent. In short, we have confirmed debromination in the S_1 states of BrAB in EtOH, BrPB@Ph in CH and BrPB@T in EtOH by observing the growth of absorption spectra of the corresponding enol forms.

3.2.2 Photochemical features of chlorinated diketones in solution

Figure 3 shows absorption spectral changes upon 254 nm photolysis of CIAB in EtOH and ACN.

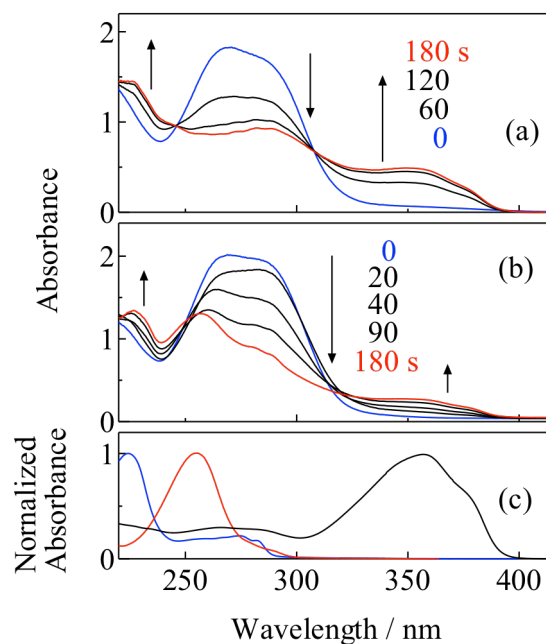
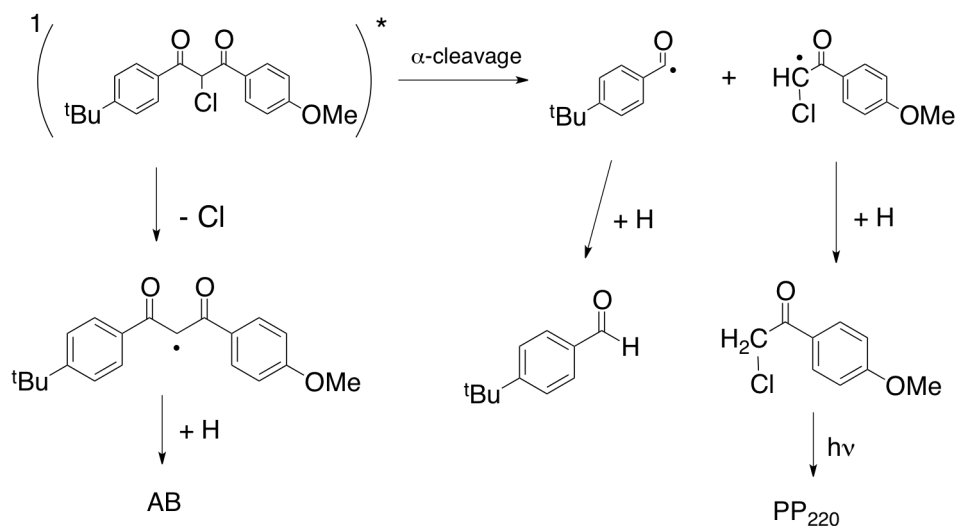


Figure 3. Absorption spectral changes upon 254 nm photolysis of CIAB in aerated EtOH (a) and ACN (b). (c) Reference absorption spectra of AB (solid), *p*-tert-butylbenzaldehyde (red) and a photoproduct (PP₂₂₀, blue) of *p*-methoxyphenacyl chloride in ACN.

In Figure 3a, with a lapse of irradiation time, the absorption band of CIAB at 274 nm decreases in EtOH with an increase of absorbance at 356 nm where AB in the enol form shows the characteristic absorption band (see Figure 3c). The AB formation indicates that dehalogenation is the major photochemical reaction of CIAB in EtOH as well as BrAB in EtOH. The quantum yield for the AB formation from CIAB in EtOH was determined to be 0.065 ± 0.01 . By contrast, features of absorption spectral changes upon photolysis of CIAB in ACN were different from those in EtOH (Figure 3b). With increasing irradiation time, the absorbance of CIAB in ACN decreases and a new absorption band was seen at 256 nm. AB formation upon photolysis of CIAB in ACN seemed to be a minor process. The quantum yield for the photodecomposition of CIAB in ACN was determined to be 0.18 ± 0.02 . Since this value was not affected by the amount of dissolved oxygen, the decomposition is the event in the S₁ state. The absorption spectrum at 180 s in Figure 3b was similar to the superposed ones of *p*-tert-butylbenzaldehyde and a photoproduct (PP₂₂₀, $\lambda_{\text{max}} = 220$ nm) of *p*-

methoxyphenacyl chloride. Absorption spectral changes upon photolysis of *p*-methoxyphenacyl chloride in ACN are displayed in the ESI (Figure S4). From these absorption spectra, it is inferred that the major photochemical reaction of CIAB in ACN is α -bond cleavage of the carbonyl (Norrish Type I) in CIAB. The plausible photochemical processes of CIAB in ACN are shown in Scheme 3.



Scheme 3. Plausible photochemical processes of CIAB.

The observed photochemical reactions are found to depend on the solvent. The H-bonding of the EtOH molecules to the carbonyl groups of CIAB may induce α -bond cleavage or prevent the C-Cl bond dissociation. Košmrlj et al. have shown that Cl-substituted DBM derivatives undergo photocyclization to form the corresponding flavones in solution via the C-Cl bond cleavage.²⁵ The quantum yield of flavone formation from 2-chloro-1,3-dibenzoylmethane was reported to be 0.022. This report is worth to be compared with our results that photocyclization from CIAB to flavone is absent in ACN instead of finding a variety of the photoproducts due to α -cleavage.

Figure 4 shows absorption spectral changes upon photolysis of CIPB@Ph in CH and ACN.

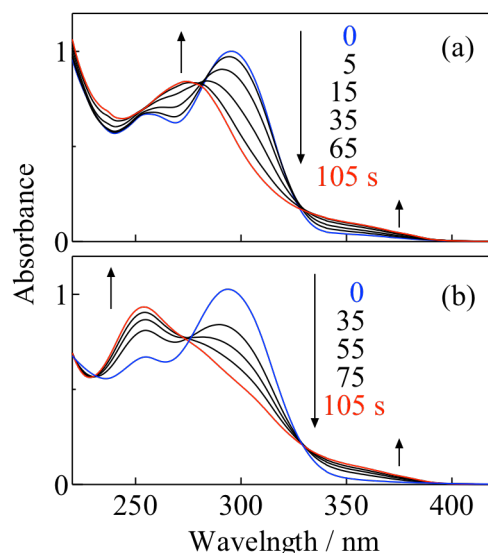
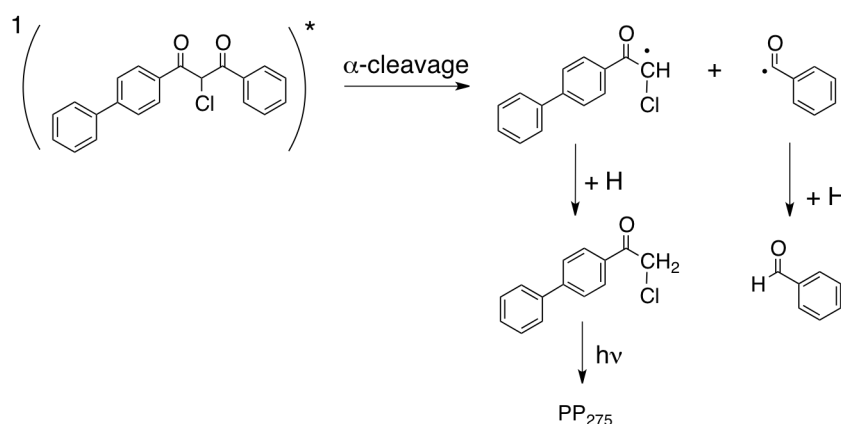


Figure 4. Absorption spectral changes upon photolysis ($\lambda > 280$ nm) of CIPB@Ph in aerated CH (a) and ACN (b).

As increasing the irradiation time, the absorption intensity of CIPB@Ph in CH decreases with isosbestic points, creating an absorption band at 275 nm (Figure 4a). The absorption spectrum obtained at 105 s agreed with the superposed ones of benzaldehyde and a photoproduct (PP_{275} , $\lambda_{\max} = 275$ nm) of *p*-phenylphenacyl chloride (See Figures S5b and c in the ESI). From these observations, the plausible primary photochemical reaction of CIPB@Ph in ACN is also suggested to be Norrish Type I depicted in Scheme 4.



Scheme 4. Plausible photochemical processes of CIPB@Ph in CH.

Photochemical reactions of CIPB@Ph in ACN (Figure 4b) were different from those in CH. The absorption spectral changes in ACN showed isosbestic points, providing a new absorption band at 253 nm, which is not due to the photoproduct ($\lambda_{\max} = 282$ nm) of *p*-phenylphenacyl chloride in ACN

(Figure S5d in the ESI). We were succeeded in isolating the photoproducts (PP₂₅₃ and PP₂₈₃) having the absorption peaks at 253 nm and 283 nm using a home-made microflow photoreactor.³⁰ The absorption spectra of PP₂₅₃ and PP₂₈₃ are deposited in the ESI as Figure S6. Unfortunately, we were unable to identify them although we have measured the mass spectra of PP₂₅₃ and PP₂₈₃ being M⁺ = 307 and 273, respectively. However, from the absence of the absorption spectrum of PB@Ph (enol form) after photolysis of ClPB@Ph in CH and ACN, it is unambiguous that occurrence of the C-Cl bond cleavage is a negligible event in the S₁ state. Conversely, We have confirmed that ClPB@F and ClPB@T undergo C-Cl bond cleavage in the S₁ state in CH and ACN. The spectral data are deposited in the ESI as Figures S7 and 8. It is interesting that the photochemical reactivity in the C-Cl bond dissociation in the diketones having the biphenyl moiety strictly depends on the counter aromatic rings (Ph, T and F).

3.3 Transient absorption measurements using laser photolysis techniques

For the purpose of understanding the photoreaction intermediates of BrAB, 266nm laser flash photolysis was performed. Figure 5a shows a transient absorption spectrum obtained upon 266 nm laser pulsing in degassed ACN solution of BrAB.

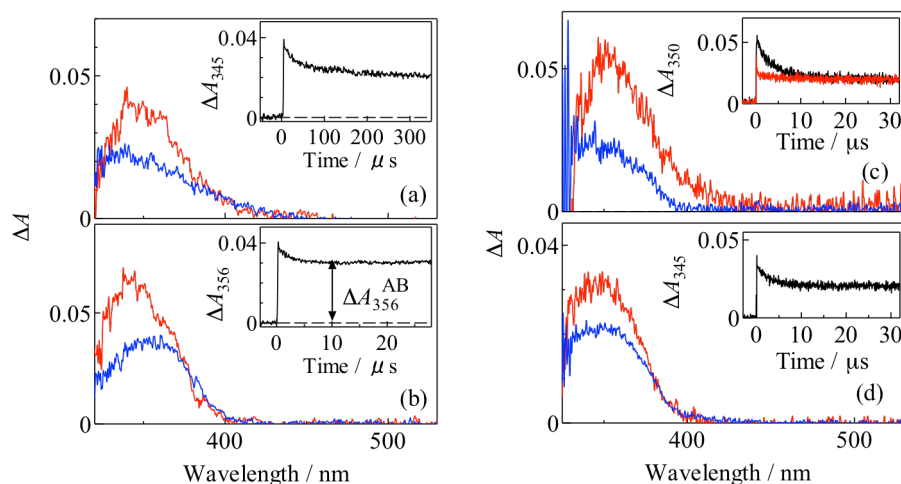


Figure 5. (a) Transient absorption spectra at 100 ns (red) and 200 μs (blue) upon 266 nm laser pulsing in ACN solution of BrAB. Insets; a temporal absorbance change at 345 nm. (b) Transient absorption spectra at 100 ns (red) and 25 μs (blue) upon 266 nm laser pulsing in EtOH solution of BrAB. Insets; a temporal absorbance change at 356 nm. (c) Transient absorption spectra at 50 ns (red) and 25 μs (blue) upon 266 nm laser pulsing in ACN solution of ClAB. Insets; temporal absorbance changes at 350 nm in degassed (solid) and aerated (red) ACN. (d) Transient absorption spectra at 50 ns (red) and 25 μs (blue) upon 266 nm laser pulsing in EtOH solution of ClAB. Insets; a temporal absorbance change at 345 nm.

The absorption spectrum at 100 ns has the absorption maximum at 345 nm, and the absorbance decreased with a rate of $2.4 \times 10^4 \text{ s}^{-1}$ (see inset in Figure 5a), providing an absorption spectrum having the maximum at 345 nm at 200 μs . We were unable to assign the species for the absorption spectrum seen at 200 μs . The shape of the incipient transient absorption spectrum at 100 ns in ACN was very similar to that obtained at 100 ns upon 266 nm laser pulsing in degassed EtOH solution of BrAB (Figure 5b). The transient absorption spectrum at 100 ns in EtOH decreases with a rate of $4.1 \times 10^5 \text{ s}^{-1}$, giving an absorption band at 356 nm at 10 μs , which is ascribable to AB on the basis of the shape and the peak wavelength. The decay rate was not affected by the amount of the dissolved oxygen. Since we have shown that stationary photolysis of BrAB in EtOH provides AB due to debromination, the absorption band at 345 nm seen at 100 ns in ACN and EtOH is probably be due to the ABR produced by debromination in the excited state of BrAB. These absorption spectrum changes of BrAB in EtOH indicate that ABR undergoes H-atom abstraction from EtOH, resulting in the formation of AB.

We have observed photochemical reactions of ClAB depending on the solvent (Scheme 3). In ACN, α -cleavage with the C-C bond predominates with a quantum yield of 0.18 whereas the

formation of AB due to the C-Cl bond dissociation proceeds in the S_1 state with a quantum yield of 0.06 in EtOH. Figure 5c shows transient absorption spectra upon laser photolysis of ClAB in ACN. The transient absorption spectrum at 350 nm decreases with a rate of $2.4 \times 10^4 \text{ s}^{-1}$, which was accelerated in the presence of the dissolved oxygen (see inset in Figure 5c). This observation indicates the presence of triplet manifold in the early stage upon photoexcitation of ClAB in ACN. The absorption of triplet ClAB may locate in the wavelength region, 320-420 nm. The absorption spectrum at 25 μs after depletion of triplet ClAB may be due to the radicals as formed by α -cleavage shown in Scheme 3. In Figure 5d, absorption spectrum obtained at 50 ns upon 266 nm laser pulsing in ClAB in EtOH resembles that obtained at 50 ns for laser photolysis of BrAB in EtOH (Figure 5b), and decayed with a rate of $3.6 \times 10^5 \text{ s}^{-1}$, giving absorption spectrum at 25 μs due to AB. The obtained decay rate for ClAB in EtOH was independent of the dissolved oxygen, and close to that ($4.1 \times 10^5 \text{ s}^{-1}$) obtained for H-atom abstraction for BrAB in EtOH. From these observations, the transient absorption changes in Figure 5d demonstrate that ABR generated by photodechlorination of ClAB undergoes H-atom abstraction from EtOH. It is notable that intersystem crossing to the triplet state of ClAB is controlled by photochemical reaction in the S_1 states influenced by H-bonding of the solvent molecules. In EtOH, dechlorination governs the S_1 state deactivation whereas intersystem crossing to the triplet competes with α -cleavage in the S_1 state in ACN.

A quantum yield, Φ_{AB} for the formation of AB upon 266 nm laser photolysis of BrAB in EtOH was determined as follows. Based on the absorbance change, ΔA for the formation of AB seen in the transient absorption at 356 nm (see inset in Figure 5c), Φ_{AB} is formulated by eqn 1.

$$\Phi_{AB} = \Delta A \varepsilon^{-1} l^{-1} (1 - 10^{-A_{266}})^{-1} I_0^{-1} \quad (1)$$

where ε , l , A_{266} and I_0 are, respectively, the molar absorption coefficient of AB at 356 nm ($32400 \text{ dm}^3 \text{ mol}^{-1} \text{ cm}^{-1}$), the optical path length (1 cm), the absorbance of BrAB at 266 nm and fluence of the incident laser pulse. The quantity of I_0 can be determined by using eqn 2 based on the quantum yield (Φ_{MC}) of photoconversion from *N*-methyldiphenylamine (MDPA) to *N*-methylcarbazole (MC) in MCH (0.42)²⁶ and the absorbance change due to the formation of MC.

$$I_0 = \Delta A_{343} \varepsilon_{MC}^{-1} l^{-1} (1 - 10^{-A_{266}^{MDPA}})^{-1} \Phi_{MC}^{-1} \quad (2)$$

Here, ΔA_{343} , ε_{MC} , l and A_{266}^{MDPA} are, respectively, the absorbance change at 343 nm due to the formation of MC, the molar absorption coefficient of MC at 343 nm ($5800 \text{ dm}^3 \text{ mol}^{-1} \text{ cm}^{-1}$)²⁶, the optical path length (1 cm) and the absorbance of MDPA at 266 nm. The actual data for ΔA and the term, $1 - 10^{-A_{266}}$ can be seen in the ESI as Figure S9. By using the slopes of these lines and eqns 1 and 2, the value of Φ_{AB} in EtOH was determined to be 0.07 ± 0.01 independent of the amount of the dissolved oxygen, which indicates that the C-Br bond cleaves in the S_1 state of BrAB. The Φ_{AB} value obtained upon laser flash photolysis is in a good agreement with that (0.08) obtained upon steady state photolysis of BrAB in EtOH. We have observed no transient absorption due to triplet BrAB in fluid solution upon laser flash photolysis. This observation convinces the efficient C-Br bond dissociation in the S_1 state, which may reduce the intersystem crossing yield to the triplet state. The similar procedure was applied to ClAB in EtOH for determining the AB formation, obtaining $\Phi_{AB} = 0.05 \pm 0.01$, which is closed to that (0.06) obtained by stationary photolysis techniques.

The decay rate ($4.1 \times 10^5 \text{ s}^{-1}$) of ABR observed for BrAB in EtOH was found to be greater than that ($k_0 = 2.3 \times 10^4 \text{ s}^{-1}$) in ACN. The quenching rate constant, k_q of ABR by EtOH was determined by obtaining decay rates, k_{obsd} at various concentrations of EtOH, [EtOH] in ACN. Figure 6 shows plots of k_{obsd} as a function of [EtOH].

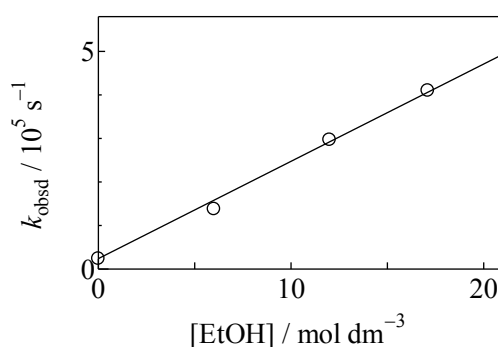


Figure 6. Decay rates (k_{obsd}) of the ABR formed upon 266 nm laser pulsing in BrAB in ACN plotted as a function of [EtOH].

Since the plots show a straight line, k_{obsd} is expressed as,

$$k_{\text{obsd}} = k_0 + k_q[\text{EtOH}] \quad (3)$$

From the slope of the line, the k_q value was determined to be $2.3 \times 10^4 \text{ dm}^3 \text{ mol}^{-1} \text{ s}^{-1}$. Since the obtained rate constant is smaller than that of the diffusion limit of ACN ($2.0 \times 10^{10} \text{ dm}^3 \text{ mol}^{-1} \text{ s}^{-1}$ at $20 \text{ }^\circ\text{C}$)³¹, it is obvious that H-abstraction of ABR proceeds in a diffusion process. Regrettably as for CIAB, because the initial photochemical reaction depended on the solvent, it was impossible to determine the rate constant for H-atom abstraction from EtOH in ACN.

We have observed that the photochemical reactions of BrPB@Ph and CIPB@Ph in CH are, respectively, debromination and α -cleavage in the S_1 states. According to these photochemical reactions, the initial species produced are to be the 4-phenylbenzoylbenzoylmethyl radical from BrPB@Ph and the 4-phenylphenacylchloromethyl and benzoyl radicals from CIPB@Ph. Laser flash photolysis was carried out to investigate the competitive reactions and formed species in these S_1 states. Figure 7 shows transient absorption spectra obtained upon 308 nm laser pulsing in the CH solution.

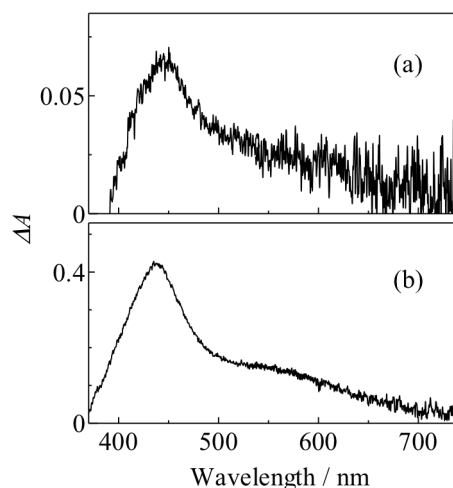


Figure 7. Transient absorption spectra obtained at 50 ns upon 308 nm laser pulsing in degassed CH solution of BrPB@Ph (a) and CIPB@Ph (b).

Transient absorption spectra having the maxima at 445 nm for BrPB@Ph and at 438 nm for CIPB@Ph were obtained. The lifetimes of these transient absorption spectra for BrPB@Ph and

CIPB@Ph in CH were, respectively, 4.7 μ s and 250 ns, and reduced by the presence of the dissolved oxygen, indicating that these transient species are ascribable to the corresponding triplet states. After depletion of the triplet-triplet (T-T) absorption spectra, no residual absorption was seen in the wavelength region of 400- 730 nm. The expected radicals formed in the S_1 states were not observed in this wavelength region, probably, located in the shorter wavelength region. It seems that no chemical reactions proceed in the T_1 states of BrPB@Ph and CIPB@Ph.

Similarly, we have obtained transient absorption spectra for BrPB@F, BrPB@F, CIPB@F and CIPB@T deposited in the ESI as Figures S10-13. The T-T absorption spectra of these compounds were observed in the wavelength region, 440- 470 nm, having the similar spectrum features to those of triplet BrPB@Ph and CIPB@Ph. The similarity in the T-T absorption spectra may be originated from the biphenyl moiety of these compounds. As with these compounds, no chemical reactions occur in the T_1 states.

3.4 Dechlorination in a highly excited triplet state studied by two-color two-laser photolysis techniques

Recently, we have been studying photochemical reactions in a highly excited triplet state of aromatic compounds using two-color two-laser photolysis techniques.³²⁻³⁶ Even if the T_1 state is free of chemical reactions, successive excitation of the T_1 state could open channel to chemical reactions in a highly excited triplet state (T_n , $n \geq 2$) because of the higher triplet energy than that of the T_1 state. In the present work, we have observed that the T_1 states of the studied diketones are inert to dehalogenation and α -cleavage, both of which were revealed to proceed in the S_1 states. We, therefore, carried out two-color (308 nm and 430 nm) two-laser flash photolysis of the diketones having the biphenyl moiety because they are found to show large absorptivities in the T-T absorption in the wavelength region, 420 - 450 nm. The first excitation of the diketone with a 308 nm laser pulse produces the T_1 state that efficiently absorbs the second laser pulse (430 nm) within the triplet lifetime. The 430 nm laser pulse is, thus, absorbed only by the triplet because the diketone

has no absorbance at 430 nm in the ground state. Figures 8a and b show absorption spectral changes after one- and two-color laser pulsing in degassed CH solution of CIPB@Ph, respectively.

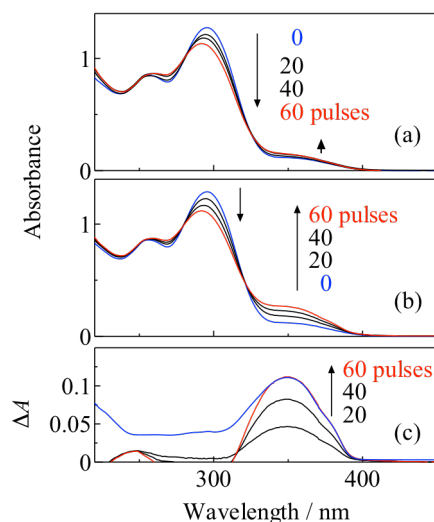


Figure 8. Absorption spectral changes upon 308 nm (a) and 308 nm plus 100 ns delayed 430 nm (b) laser pulsing in degassed CH solution of CIPB@Ph. (c) Differential absorption spectra between those in Figure 8a and b at the same number of laser pulses. The blue absorption spectrum is of PB@Ph in CH.

When one-color (308 nm) laser pulses are irradiated in the solution (Figure 8a), the absorption band at 350 nm displays very small changes in the absorbance. In the presence of the 100 ns-delayed second laser (430 nm) pulses, definite increases in absorbance at 350 nm can be seen as increasing the number of the laser pulse. Figure 8c shows the difference absorption spectra between ones in the absence and the presence of the second laser pulsing, The shape of the absorption spectrum at 350 nm exactly agreed with that of PB@Ph in CH, indicating that the second laser excitation caused dechlorination in a T_n state of CIPB@Ph. Unfortunately, quantum yields for dechlorination in a T_n state were too small to determine with laser photolysis techniques. Similar dechlorination in a T_n state was found for CIPB@F and CIPB@T in CH using two-color two-laser photolysis techniques. The spectral data are shown in Figures S14 and 15 in the ESI. We tried to examine debromination in T_n states of BrPB@Ph, BrPB@F and BrPB@T in CH. However, because of small absorbance of the T_1 states, we were unable to obtain definite increases in absorbance for the debrominated enols in the difference spectra such as Figure 8c. The reaction mechanism for Cl elimination in the T_n states is discussed in the next section.

3.5 Bond dissociation energies based on the heats of formation calculated by DFT computation

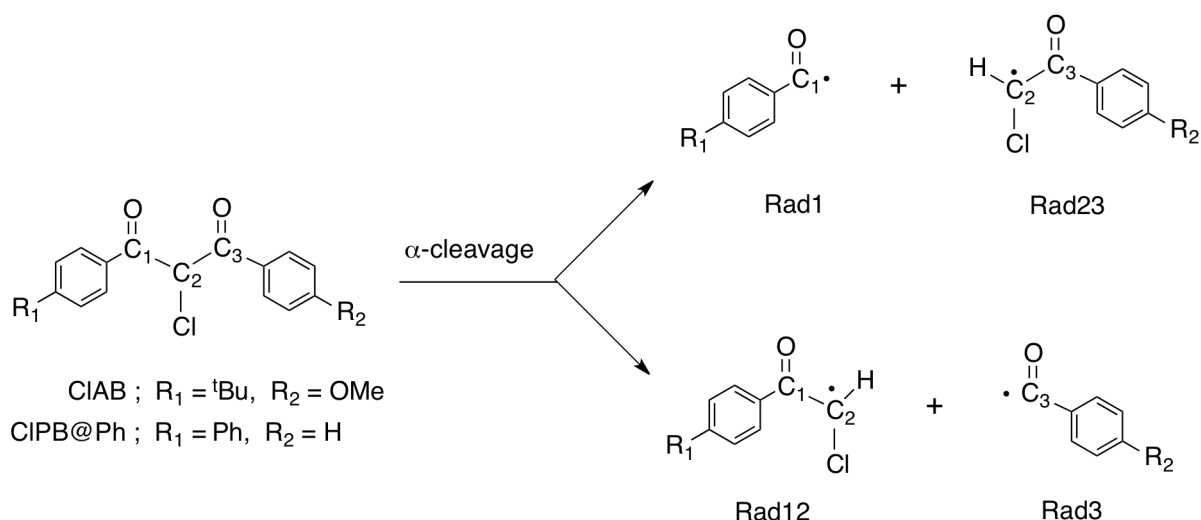
The bond dissociation energies, BDE(C-X) of the C-X (X = Br and Cl) bond in the studied diketones were evaluated on the basis of the heat of formation ($\Delta_f H$) for halide diketones (XDK), diketone radicals (DKR) and halide atoms (X) evaluated by the DFT calculations at the UB3LYP/6-31G(d) level. It is plausible that the molecular configuration of DKR is of a methyl-radical type immediately after C-X bond dissociation. The BDE(C-X) value was estimated by using eqn 4.

$$\Delta_f H(\text{XDK}) = \Delta_f H(\text{DKR}) + \Delta_f H(\text{X}) - \text{BDE}(\text{C-X}) \quad (4)$$

The estimated BDE values are listed in Table 2. The calculated $\Delta_f H$ values are deposited in Tables S1 and 2 in the ESI. The BDE(C-Cl) value of the XDK is greater than that of BDE(C-Br) by 3 - 5 kcal mol⁻¹. We have recognized debromination of BrDK in the S₁ state from the absorption spectral changes as well as dechlorination in the S₁ states of ClDK except ClPB@Ph. It is obvious that the calculated BDE(C-X) values are substantially smaller than the S₁ state energies of XDK. Thus, the dehalogenation processes possibly proceed in the S₁ states depending on the variety of the solvent. Conversely, no dehalogenation in the triplet state of XDK having the biphenyl moiety was found in the present study. From the energetic viewpoint, it is understandable that the triplet state is inactive to dehalogenation because the triplet energies (ca. 60 kcal mol⁻¹) of these XDKs are close to or smaller than the BDE(C-X) values. On the other hand, we have demonstrated by two-color two-laser photolysis techniques that excitation of the T₁ state to the T_n state enables to dissociate the C-Cl bond of ClDK having the biphenyl moiety. Since absorbing the second laser pulse (430 nm) in the T₁ state will elevate the triplet state energy by ca. 66 kcalmol⁻¹, the T_n state will locate at ca. 126 kcalmol⁻¹. Internal conversion from the T_n state will form a highly excited triplet state, T_r that is allowed to have interaction with a dissociative potential for the C-Cl bond via avoided crossing,³⁷ leading to Cl elimination.

As with ClAB and ClPB@Ph, occurrence of α -cleavage (C-C bond dissociation) in the S₁ states was found based on the absorption spectrum observations. The dissociated C-C bonds were identified as shown in Schemes 3 and 4 although the keto-formed diketones have two cleavable α -C-

C bonds by Norrish Type I reaction. Possible reaction processes providing C-radicals (Rad1, Rad23, Rad12 and Rad3) as the primary products by α -cleavage in CIAB and CIPB@Ph are depicted in Scheme 5.



Scheme 5. Possible pathways of α -cleavage in CIAB and CIPB@Ph with numbered carbon atoms.

The BDE(C-C) for the α -C-C bond was evaluated using eqns 5 and 6, and the $\Delta_f H$ values for the C-radicals calculated with DFT computation.

$$\Delta_f H(\text{XDK}) = \Delta_f H(\text{Rad1}) + \Delta_f H(\text{Rad23}) - \text{BDE}(\text{C}_1\text{-C}_2) \quad (5)$$

$$\Delta_f H(\text{XDK}) = \Delta_f H(\text{Rad12}) + \Delta_f H(\text{Rad3}) - \text{BDE}(\text{C}_2\text{-C}_3) \quad (6)$$

The calculated $\Delta_f H$ values are deposited in Table S3 in the ESI along with those for CIPB@F and CIPB@T where we have not recognized α -cleavage in CH, but Cl elimination from the absorption spectral changes (Figure S8). The imaginary pathways for α -cleavage of CIPB@T and CIPB@F are shown in Scheme S1 in the ESI. The estimated BDE(C-C) values are listed in Table 3. The difference in the evaluated BDE(C-C) values for CIAB and CIPB@Ph is very small and similar. The BDE(C₁-C₂) (= 61.8 kcal mol⁻¹) for the actually cleavable bond in CIAB is very close to the BDE(C-Cl) (= 61.7 kcal mol⁻¹). The small difference between these BDEs enables to alter the photochemical reactions, α -cleavage and dechlorination by the solvent properties, probably the ability of H-bonding to the carbonyl groups of CIAB. By contrast, the BDE(C-C) (= 59.8 kcal mol⁻¹) is appreciably small

enough to predominate α -cleavage in the S_1 state of CIPB@Ph, resulting the absence of dechlorination with BDE(C-Cl) (= 62.9 kcal mol⁻¹). As with CIPB@F and CIPB@T, both or either of the BDE(C-C) values are smaller than the BDE(C-Cl) although we have observed Cl elimination in the S_1 state. We are unable to predict photochemical reactions of CIPB@F and CIPB@T from the energetic viewpoint.

4. Conclusion

Six halogenated diketones were prepared, and the photophysical and photochemical processes in various solvents were studied by stationary and laser flash photolyses. From the absorption spectral features, the molecular structures of the prepared halogenated diketones were revealed to be in the keto form in the solvents except for BrPB@F and CIPB@F in EtOH where the enol form may be to a small extent in equilibrium with the keto form. The excited singlet and triplet state energies were determined from the absorption and emission spectra. From the absorption spectral changes upon steady state photolysis of brominated diketones in EtOH, Br elimination was found to be the major primary photochemical process to form the corresponding halogen-free diketones. The determined quantum yields for the formation of the halogen-free diketones were independent of the amount of the dissolved oxygen, indicating that the C-Br bond cleavage occurs in the S_1 states. The estimated BDE(C-Br) values based on the DFT calculation were smaller than the S_1 energies. Conversely, from the absorption spectra of photoproducts upon photolysis of CIAB and CIPB@Ph, it was inferred that Norrish type I is the primary major photochemical reaction in the S_1 states in ACN. CIPB@F and CIPB@T were found to undergo dechlorination in the S_1 states in CH because the formation of PB@F and PB@T was, respectively, observed in the absorption spectral changes. Laser photolysis studies of BrAB in ACN and EtOH provided a transient absorption spectrum ascribable to ABR as the initial intermediate due to the Br elimination, followed by the AB formation in EtOH. These observations provide evidence that H-atom abstraction of ABR from EtOH is responsible for the AB formation. The determined quenching rate constant of ABR by EtOH was smaller than the

diffusion limit of ACN. Conversely, laser flash photolysis of brominated and chlorinated PB@Ph, PB@F and PB@T showed the T-T absorption. No chemical reactions in these T_1 states were found. The great absorptivities of triplet CIPB@Ph, CIPB@F and CIPB@T allowed us to carry out two-color two-laser photolysis studies, resulting in the formation of the corresponding halogen-free diketones in CH in the presence of the second laser pulsing. These observations convinced occurrence of Cl elimination in the T_n ($n \geq 2$) states. The reaction mechanism for Cl elimination in the T_n states is discussed. Unfortunately, we were unable to determine the quantum yields for the C-Cl bond dissociation in the T_n state. We conclude that the photochemical reactions of the studied XDKs are strongly dependent on the varieties of the halogen atom, aromatic rings, solvents and the spin multiplicities of the excited states.

Acknowledgments This work has been supported by a Grant-in-Aid for Scientific Research (26288032) from the Ministry of Education, Culture, Sports, Science and Technology (MEXT) of Japanese Government. MY thanks Cosmetogy Foundation for the financial support. Prof. Teruo Shinmyozu and Dr. Kenta Goto at Kyusyu University are acknowledged for performing the mass spectroscopy of PP₂₅₃ and PP₂₈₃.

Electronic Supplementary Information (ESI) available: Absorption and emission spectra, absorption spectral changes upon steady photolysis, transient absorption spectra and results of DFT calculation for the heat of formation.

Notes and References

1. P. Gacoin, Studies of the Triplet State of Carbonyl Compounds. I. Phosphorescence of β -Diketones, *J. Chem. Phys.*, 1972, **57**, 1418-1425.
2. A. J. Vila, C. M. Lagier and A. C. Olivieri, Proton transfer in solid 1-phenylbutane-1,3-dione and related 1,3-diones as studied by carbon-13 CPMAS NMR spectroscopy and AM1 calculations, *J. Phys. Chem.*, 1991, **95**, 5069-5073.
3. H. Gonzenbach, T. J. Hill and T. G. Truscott, The triplet energy levels of UVA and UVB sunscreens, *Journal of Photochemistry and Photobiology B: Biology*, 1992, **16**, 377-379.
4. N. M. Roscher, M. K. O. Lindemann, S. Bin Kong, C. G. Cho and P. Jiang, Photodecomposition of several compounds commonly used as sunscreen agents, *J. Photochem. Photobiol. A: Chem.*, 1994, **80**, 417-421.

5. W. Schwack and T. Rudolph, Photochemistry of dibenzoyl methane UVA filters Part 1, *J. Photochem. Photobiol. B: Biol.*, 1995, **28**, 229-234.
6. I. Andrae, A. Bringham, F. Böhm, H. Gonzenbach, T. Hill, L. Mulroy and T. G. Truscott, A UVA filter (4-*tert*-butyl-4'-methoxydibenzoylmethane): photoprotection reflects photophysical properties, *J. Photochem. Photobiol. B: Biol.*, 1997, **37**, 147-150.
7. M. Dubois, P. Gilard, P. Tiercet, A. Deflandre and M. A. Lefebvre, Photoisomerisation of the sunscreen filter PARSOL®1789, *J. Chim. Phys.*, 1998, **95**, 388-394.
8. F. P. Gasparro, M. Mitchnick and J. F. Nash, A review of sunscreen safety and efficacy, *Photochem. Photobiol.*, 1998, **68**, 243-256.
9. A. Cantrell and D. J. McGarvey, Photochemical studies of 4-*tert*-butyl-4'-methoxydibenzoylmethane (BM-DBM), *J. Photochem. Photobiol. B: Biol.*, 2001, **64**, 117-122.
10. C. Eric and G. Bernard, Photostabilization of butyl methoxydibenzoylmethane (avobenzone) and ethylhexyl methoxycinnamate by bis-ethylhexyloxyphenol methoxyphenyl triazine (Tinosorb S), a new UV broadband filter, *Photochem. Photobiol.*, 2001, **74**, 401-406.
11. F. Wetz, C. Routaboul, D. Lavabre, J.-C. Garrigues, I. Rico-Lattes, I. Pernet and A. Denis, Photochemical behavior of a new long-chain UV absorber derived from 4-*tert*-butyl-4'-methoxydibenzoylmethane, *Photochem. Photobiol.*, 2004, **80**, 316-321.
12. E. Damiani, L. Rosati, R. Castagna, P. Carloni and L. Greci, Changes in ultraviolet absorbance and hence in protective efficacy against lipid peroxidation of organic sunscreens after UVA irradiation, *J. Photochem. Photobiol. B: Biol.*, 2006, **82**, 204-213.
13. D. Dondi, A. Albin and N. Serpone, Interactions between different solar UVB/UVA filters contained in commercial suncreams and consequent loss of UV protection, *Photochem. Photobiol. Sci.*, 2006, **5**, 835-843.
14. A. Aspée, C. Aliaga and J. C. Scaiano, Transient enol isomers of dibenzoylmethane and avobenzone as efficient hydrogen donors toward a nitroxide pre-fluorescent probe, *Photochem. Photobiol.*, 2007, **83**, 481-485.
15. E. Damiani, W. Baschong and L. Greci, UV-Filter combinations under UV-A exposure: Concomitant quantification of over-all spectral stability and molecular integrity, *J. Photochem. Photobiol. B: Biol.*, 2007, **87**, 95-104.
16. S. P. Huong, E. Rocher, J.-D. Fourneron, L. Charles, V. Monnier, H. Bun and V. Andrieu, Photoreactivity of the sunscreen butylmethoxydibenzoylmethane (DBM) under various experimental conditions, *J. Photochem. Photobiol. A: Chem.*, 2008, **196**, 106-112.
17. G. J. Mturi and B. S. Martincigh, Photostability of the suncreening agent 4-*tert*-butyl-4'-methoxydibenzoylmethane (avobenzone) in solvents of different polarity and proticity, *J. Photochem. Photobiol. A: Chem.*, 2008, **200**, 410-420.
18. C. Paris, V. Lhiaubet-Vallet, O. Jiménez, C. Trullas and M. Á. Miranda, A blocked diketo form of avobenzone: Photostability, photosensitizing properties and triplet quenching by a triazine-derived UVB-filter, *Photochem. Photobiol.*, 2009, **85**, 178-184.
19. M. Yamaji and M. Kida, Photothermal Tautomerization of a UV Sunscreen (4-*tert*-butyl-4'-methoxydibenzoylmethane) in acetonitrile studied by steady-state and laser flash photolysis, *J. Phys. Chem. A*, 2013, **117**, 1946-1951.
20. N. Oguchi-Fujiyama, K. Miyazawa, A. Kikuchi and M. Yagi, Photophysical properties of dioctyl 4-methoxybenzylidenemalonate: UV-B absorber, *Photochem. Photobiol. Sci.*, 2012, **11**, 1528-1535.
21. M. Yamaji, C. Paris and M. Á. Miranda, Steady-state and laser flash photolysis studies on photochemical formation of 4-*tert*-butyl-4'-methoxydibenzoylmethane from its derivative via the Norrish Type II reaction in solution, *J. Photochem. Photobiol. A: Chem.*, 2010, **209**, 153-157.
22. M. Yamaji, S. Wakabayashi, S. Ueda, H. Shizuka and S. Tobita, Laser photolysis studies of endoergic triplet energy transfer in solution by observing the carbon-sulfur bond cleavage of triplet-sensitized naphthylmethyl phenyl sulfide, *Chem. Phys. Lett.*, 2003, **368**, 41-48.

23. E. Cogné-Laage, J.-F. Allemand, O. Ruel, J.-B. Baudin, V. Croquette, M. Blanchard-Desce and L. Jullien, Diaroyl(methanato)boron difluoride compounds as medium-sensitive two-photon fluorescent probes, *Chem. Eur. J.*, 2004, **10**, 1445-1455.
24. J. Košmrlj, M. Kočevar and S. Polanc, A new convenient bromination with $\text{KBrO}_3/\text{KBr}/\text{Dowex}^\circledast$, *Synth. Commun.*, 1996, **26**, 3583-3592.
25. B. Kosmrlj and B. Sket, Photocyclization of 2-chloro-substituted 1,3-diarylpropan-1,3-diones to flavones, *Org. Lett.*, 2007, **9**, 3993-3996.
26. E. W. Förster, K. H. Grellman and H. Linschitz, Reaction patterns and kinetics of the photoconversion of *N*-methyldiphenylamine to *N*-methycarbazole, *J. Am. Chem. Soc.*, 1973, **95**, 3108-3115.
27. M. Hoshino and M. Koizumi, Order of quencher participation in Photochemistry. I. Proton transfer from the excited *p*-hydroxybenzophenone in mixed solvents of cyclohexane and alcohols, *Bull. Chem. Soc. Jpn.*, 1972, **45**, 2731-2736.
28. M. Yamaji, Y. Aihara, T. Itoh, S. Tobita and H. Shizuka, Thermochemical profiles on hydrogen atom transfer from triplet naphthol and proton-induced electron transfer from triplet methoxynaphthalene to benzophenone via triplet exciplexes studied by laser flash photolysis, *J. Phys. Chem.*, 1994, **98**, 7014-7021.
29. M. J. Frisch, G. W. Trucks, H. B. Schlegel, G. E. Scuseria, M. A. Robb, J. R. Cheeseman, G. Scalmani, V. Barone, B. Mennucci, G. A. Petersson, H. Nakatsuji, M. Caricato, X. Li, H. P. Hratchian, A. F. Izmaylov, J. Bloino, G. Zheng, J. L. Sonnenberg, M. Hada, M. Ehara, K. Toyota, R. Fukuda, J. Hasegawa, M. Ishida, T. Nakajima, Y. Honda, O. Kitao, H. Nakai, T. Vreven, J. J. A. Montgomery, J. E. Peralta, F. Ogliaro, M. Bearpark, J. J. Heyd, E. Brothers, K. N. Kudin, V. N. Staroverov, T. Keith, R. Kobayashi, J. Normand, K. Raghavachari, A. Rendell, J. C. Burant, S. S. Iyengar, J. Tomasi, M. Cossi, N. Rega, J. M. Millam, M. Klene, J. E. Knox, J. B. Cross, V. Bakken, C. Adamo, J. Jaramillo, R. Gomperts, R. E. Stratmann, O. Yazyev, A. J. Austin, R. Cammi, C. Pomelli, J. W. Ochterski, R. L. Martin, K. Morokuma, V. G. Zakrzewski, G. A. Voth, P. Salvador, J. J. Dannenberg, S. Dapprich, A. D. Daniels, O. Farkas, J. B. Foresman, J. V. Ortiz, J. Cioslowski and D. J. Fox, Gaussian 09, Revision C.01, Gaussian, Inc., Wallingford CT, 2010.
30. H. Okamoto, T. Takane, S. Gohda, Y. Kubozono, K. Sato, M. Yamaji and K. Satake, Efficient synthetic photocyclization for phenacenes using a continuous flow reactor, *Chem. Lett.*, 2014, **43**, 994-996.
31. S. L. Murov, I. Carmichael and G. L. Hug, *Handbook of Photochemistry, Second Edition, Revised and Expanded*, Marcel Dekker, Inc. New York, Second Edition, Revised and Expanded edn., 1993.
32. M. Yamaji, A. Kojima and S. Tobita, Stepwise laser photolysis studies of β -bond cleavage in highly excited triplet states of biphenyl derivatives having C-O bonds, *J. Phys. Chem. A*, 2007, **111**, 770-776.
33. M. Yamaji, Stepwise two-color laser photolysis studies of α -cleavage in highly excited triplet states of α -acyl-4-phenylphenols, *Photochem. Photobiol. Sci.*, 2008, **7**, 711-717.
34. M. Yamaji, X. Cai, M. Sakamoto, M. Fujitsuka and T. Majima, Photodecomposition profiles of β -bond cleavage of phenylphenacyl derivatives in the higher triplet excited states during stepwise two-color two-laser flash photolysis, *J. Phys. Chem. A*, 2008, **112**, 11306-11311.
35. M. Yamaji, X. Cai, M. Sakamoto, M. Fujitsuka and T. Majima, α -Bond dissociation of *p*-phenylbenzoyl derivatives in the higher triplet excited state studied by two-color two-laser flash photolysis, *J. Phys. Chem. A*, 2009, **113**, 1696-1703.
36. V. Vendrell-Criado, G. M. Rodríguez-Muñiz, M. Yamaji, V. Lhiaubet-Vallet, M. C. Cuquerella and M. A. Miranda, Two-photon chemistry from upper triplet states of thymine, *J. Am. Chem. Soc.*, 2013, **135**, 16714-16719.
37. W. G. Dauben, L. Salem and N. J. Turro, A classification of photochemical reactions, *Acc. Chem. Res.*, 1975, **8**, 41-54.

Table 1. Absorption properties and excited state energies of aromatic 1,3-diketones used in the present work.

Compound	$\lambda_{\max} / \text{nm}$ ($\epsilon / \text{dm}^3 \text{mol}^{-1} \text{cm}^{-1}$)	$E_S^a / \text{kcal mol}^{-1}$	$E_T^b / \text{kcal mol}^{-1}$
AB	356 (32400) ^c	72.6	58.4
BrAB	270 (22100) ^c	~77	68.3
ClAB	270 (23500) ^c	~77	68.5
PB@Ph	354 (33600) ^d	73.8	57.9
BrPB@Ph	295 (25500) ^d	~75	59.5
ClPB@Ph	295 (25400) ^d	~75	59.7
PB@F	366 (32600) ^c	71.9	57.1
	363 (40700) ^d		
BrPB@F	287 (32500) ^c	~75	59.5
ClPB@F	288 (32600) ^c	~75	59.2
PB@T	368 (34400) ^c	71.3	56.0
	362 (36300) ^d		
BrPB@T	298 (28000) ^c	~76	62.2
ClPB@T	296 (31000) ^c	~76	62.2

a) For AB, PB@Ph, PB@F and PB@T, estimated as an averaged energy based on the 0-0 origins of the absorption and fluorescence spectra in ACN at 295 K while for the others, from the onset wavelength of the absorption spectrum. b) Determined from the 0-0 origin of the corresponding phosphorescence spectrum in EtOH at 77 K. c) In acetonitrile. d) In cyclohexane.

Table 2. Bond dissociation energies, BDE (C-X)^a.

XDK	BDE (C-Br)	BDE (C-Cl)
XAB	57.4	61.7
XPB@Ph	58.6	62.9
XPB@F	60.1	65.0
XPB@T	58.9	62.3

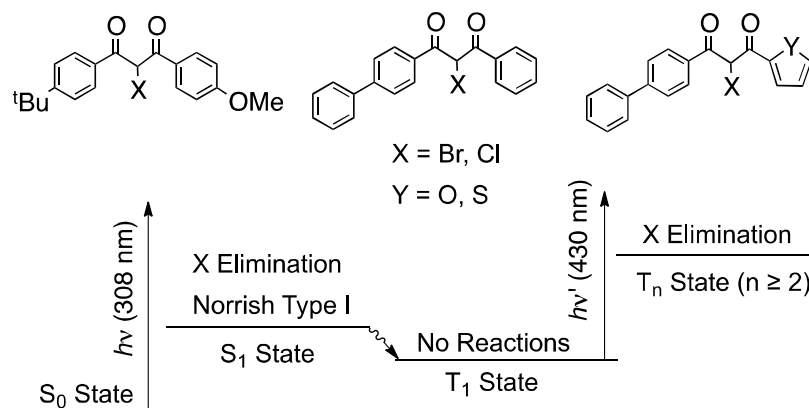
a) In kcal mol⁻¹. Evaluated by eqn 4.

Table 3. Bond dissociation energies, BDE (C-C)^a.

CIDK	BDE (C ₁ -C ₂)	BDE (C ₂ -C ₃)
CIAB	61.8	(61.4)
CIPB@Ph	(59.8)	59.8
CIPB@F	(62.1)	(61.8)
CIPB@T	(60.5)	(128.0)

a) In kcal mol⁻¹. Evaluated by eqns 5 and 6.
The values in parentheses are for imaginary cleavage.

Graphic Abstract



Photoreactions of 1,3-diketones having halogen atoms at the C2 position are investigated by steady state, one- and two-color laser photolyses and DFT calculation.